

Effect of chemical inhomogeneity in the bismuth-based copper oxide superconductors

H.Eisaki,* N. Kaneko,† D.L. Feng,‡ A. Damascelli,§ P.K. Mang, K.M. Shen, Z.-X. Shen, and M. Greven

*Department of Applied Physics, Physics, and Stanford Synchrotron
Radiation Laboratory, Stanford University, Stanford CA, 94305*

(Dated: November 1, 2018)

We examine the effect on the superconducting transition temperature (T_c) of chemical inhomogeneities in $\text{Bi}_2\text{Sr}_2\text{CuO}_{6+\delta}$ and $\text{Bi}_2\text{Sr}_2\text{CaCu}_2\text{O}_{8+\delta}$ single crystals. Cation disorder at the Sr crystallographic site is inherent in these materials and strongly affects the value of T_c . Partial substitution of Sr by Ln (Ln = La, Pr, Nd, Sm, Eu, Gd, and Bi) in $\text{Bi}_2\text{Sr}_{1.6}\text{Ln}_{0.4}\text{CuO}_{6+\delta}$ results in a monotonic decrease of T_c with increasing ionic radius mismatch. By minimizing Sr site disorder at the expense of Ca site disorder, we demonstrate that the T_c of $\text{Bi}_2\text{Sr}_2\text{CaCu}_2\text{O}_{8+\delta}$ can be increased to 96 K. Based on these results we discuss the effects of chemical inhomogeneity in other bulk high-temperature superconductors.

PACS numbers: 74.62.-c, 74.62.Bf, 74.62.Dh, 74.72.Hs

I. INTRODUCTION

The possible existence of nanoscale electronic inhomogeneity — the propensity of charge carriers doped into the CuO_2 plane to form nanoscale structures — has drawn much attention in the field of high- T_c superconductivity. Neutron scattering studies on Nd co-doped $\text{La}_{2-x}\text{Sr}_x\text{CuO}_4$ (Nd-LSCO)¹ and STM/STS studies on $\text{Bi}_2\text{Sr}_2\text{CaCu}_2\text{O}_{8+\delta}$ (Bi2212)² have led to suggestions that such self-organization may manifest itself as one-dimensional “stripes” in Nd-LSCO, or two-dimensional “patches” in Bi2212. In the former case, the inter-stripe spacing in the superconducting regime is reported to be approximately four times the in-plane lattice constant, about 1.5 nm, and in the latter case the patches are estimated to be 1-3 nm across. Many theoretical studies suggest that the spatial electronic inhomogeneity in the hole-doped CuO_2 planes is an essential part of high- T_c physics³. However, at present, the importance of, or even the existence of generic nanoscale electronic inhomogeneity remains controversial^{4,5}.

If nanoscale electronic inhomogeneity exists in the superconducting cuprates, the doped holes will distribute themselves in the CuO_2 planes so as to minimize their total energy. In real materials, the CuO_2 planes are usually inhomogeneous due to local lattice distortions and/or the random Coulomb potential resulting from chemical disorder, which differs from system to system. Therefore, even if electronic inhomogeneity may itself be a genuine property of doped CuO_2 planes, the spatial variation of doped holes will likely depend on the details of each material. For example, in the framework of the stripe model¹, incommensurate spin and charge correlations are stabilized in Nd-LSCO by the long-range distortion of the CuO_6 octahedra in the low-temperature tetragonal phase, which creates one-dimensional potential wells. For Bi2212, it is argued that the random Coulomb potential caused by excess oxygen atoms in the BiO planes pins the doped holes, thus creating patch-shaped inhomogeneities². These observations suggest that *electronic and chemical inhomogeneity are inseparable from each other*, and that the un-

derstanding of the latter is imperative for an understanding of the former.

Motivated by this line of reasoning, we have examined the effects of chemical inhomogeneity in single-layer $\text{Bi}_2\text{Sr}_2\text{CuO}_{6+\delta}$ (Bi2201) and double-layer Bi2212. Although widely used for surface sensitive measurements such as STM² and angle-resolved photoemission spectroscopy (ARPES)⁶, a detailed understanding of their materials properties is very limited, when compared to other materials such as LSCO or $\text{YBa}_2\text{Cu}_3\text{O}_{7-\delta}$.

The Bi-based cuprates contain excess oxygens in BiO planes and one can change their carrier concentration by changing the amount, δ . The excess oxygen would engender a random Coulomb potential in the CuO_2 planes. Besides the oxygen nonstoichiometry in BiO planes, there exists another source of chemical inhomogeneity which inherently exists in typical samples. Although referred to as Bi2201 and Bi2212, it is empirically known that stoichiometric $\text{Bi}_{2.0}\text{Sr}_{2.0}\text{CuO}_{6+\delta}$ and $\text{Bi}_{2.0}\text{Sr}_{2.0}\text{CaCu}_2\text{O}_{8+\delta}$ are very difficult to synthesize^{7,8}, even in a polycrystalline form. In order to more easily form the crystal structure, one usually replaces Sr^{2+} ions by trivalent ions, such as excess Bi^{3+} ions or La^{3+} ions, forming $\text{Bi}_{2+x}\text{Sr}_{2-x}\text{CuO}_{6+\delta}$, $\text{Bi}_2\text{Sr}_{2-x}\text{La}_x\text{CuO}_{6+\delta}$, and $\text{Bi}_{2+x}\text{Sr}_{2-x}\text{CaCu}_2\text{O}_{8+\delta}$. As listed up in Ref. 9, a typical Bi:Sr nonstoichiometry, x , for Bi2212 is around 0.1, which yields a $T_c=89\text{-}91\text{K}$. To our knowledge, the highest T_c reported in the literature is 95K (Ref.9 (g),(i)). For Bi2201, T_c of $\text{Bi}_{2+x}\text{Sr}_{2-x}\text{CuO}_{6+\delta}$ is around 10K for $x(\text{Bi})=0.1$, whereas La substituted Bi2201 ($\text{Bi}_2\text{Sr}_{2-x}\text{La}_x\text{CuO}_{6+\delta}$) has a higher $T_c >30\text{K}$ for $x(\text{La})\approx 0.4$ ¹⁰. Since the Sr atom is located next to the apical oxygen which is just above the Cu atoms, the effect of Sr site (also referred to as the A-site) cation inhomogeneity is expected to be stronger than that of the excess oxygens in BiO planes. Note that BiO planes are located relatively far away from CuO_2 planes, with SrO planes in between.

In this study, we evaluate the effect of chemical inhomogeneity in the Bi-based cuprates. For Bi2201, we have grown a series of $\text{Bi}_2\text{Sr}_{1.6}\text{Ln}_{0.4}\text{CuO}_{6+\delta}$ crystals with var-

ious trivalent rare earth (Ln) ions. In this series, the magnitude of the local lattice distortion can be changed systematically by making use of the different ionic radii of the substituted Ln ions. We find that T_c monotonically decreases with increasing ionic radius mismatch. For Bi2212, a series of $\text{Bi}_{2+x}\text{Sr}_{2-x}\text{CaCu}_2\text{O}_{8+\delta}$ crystals with varying values of x were grown in order to evaluate the effect of Bi:Sr nonstoichiometry. In addition, we also have grown $\text{Bi}_2\text{Sr}_2\text{Ca}_{1-y}\text{Y}_y\text{Cu}_2\text{O}_{8+\delta}$, and find that substitution of Y for Ca site helps to enforce Bi:Sr stoichiometry and to raise T_c to 96 K for $y = 0.08$.

Our results demonstrate that the cation disorder, in particular that located at the Sr site, significantly affects the maximum attainable $T_c(T_{c,\text{max}})$ in the Bi-based superconductors. In order to explain our results we use a conceptual hierarchy that classifies and ranks the principal kinds of chemical disorder possible in these systems. We then extend our arguments to other cuprates to examine whether a general trend exists in the hole-doped high- T_c superconductors.

This paper is organized as follows: Section II contains detailed information about sample preparation and characterization. The experimental results are presented in Section III and discussed in Section IV, while the effects of disorder in other cuprates is addressed in Section V.

II. SAMPLE PREPARATION

Single crystals of Bi2201 and Bi2212 were grown using the travelling-solvent floating-zone technique, which is now the preferred method for synthesizing high-purity single crystals of many transition metal oxides. This technique allows for greater control of the growth conditions than is possible either by standard solid state reactions or by the flux method.

Powders of Bi_2O_3 , SrCO_3 , CaCO_3 , Ln_2O_3 (Ln=La, Pr, Nd, Sm, Eu, Gd, Y), and CuO (all of 99.99% or higher purity) were well dried and mixed in the desired cation ratio (Bi:Sr:Ln:Cu=2 : 2 - x : x : 1 for Bi2201 and Bi:Sr:Ca:Cu=2 + x : 2 - x : 1 : 2 for Bi2212), and then repeatedly calcinated at about 800°C with intermediate grinding. Eventually, the powder was finely ground and formed into a 100 mm long rod with a diameter of 5 mm. The crystal growth was performed using a Crystal Systems Inc. infrared radiation furnace equipped with four 150 W halogen lamps. Except for nearly-stoichiometric ($x = 0$) Bi2212, the rods were premelted at 18 mm/h to form dense feed rods. The crystal growth was carried out without the use of a solvent and at a growth speed of 0.3-0.4 mm/h for Bi2201 and 0.15-0.2 mm/h for Bi2212. The growth atmospheres adopted for the Bi2212 growth are listed in Table 1. Bi2201 single crystals were grown in 1 atm of flowing O_2 .

The growth condition for the $x = 0$ Bi2212 sample was more stringent than for the other samples. In order to obtain homogeneous polycrystalline feed rods, a mixture of starting powders with the stoichiometric ra-

tio Bi:Sr:Ca:Cu=2:2:1:2 was calcinated in stages, at temperatures increasing from 770°C to 870°C in 10°C increments, with intermediate grindings. The final calcination temperature (870°C) was set to be just below the composition's melting temperature (875°C). The duration of each calcination was about 20 hours. To avoid possible compositional fluctuation in the feed rod, instead of premelting, the feed rod was sintered four times in the floating-zone furnace at a speed of 50 mm/h. This process allowed us to obtain dense feed rods, approximately 95% of the ideal density. The atmosphere required for stable crystal growth was $7 \pm 3\% \text{ O}_2$, a range much narrower than for nonstoichiometric or Y-doped Bi2212. The grown crystal rod contained small amounts of a single-crystalline SrCuO_2 secondary phase, indicating that the sample still suffers from Bi:Sr nonstoichiometry. Single-phase Bi2212 single crystals could be cleaved from the grown rod. No traces of impurity phases were found in other compositions.

Inductively coupled plasma (ICP) spectroscopy was carried out to determine the chemical compositions of the crystals. Additional electron-probe microanalysis (EPMA) was also carried out on the Bi2201 crystals. The results confirm that the actual compositions follow the nominal compositions, as listed in Table 1 for Bi2212. Hereafter, we basically denote the samples by nominal composition to avoid confusion. In order to determine the maximum T_c for each cation composition (i.e., to achieve optimal hole concentration), the Bi2212 samples were annealed at various temperatures and oxygen partial pressures using a tube furnace equipped with an oxygen monitor and a sample transfer arm, which allowed us to rapidly quench the annealed samples from high temperatures within a closed environment. This procedure ensures that the variation of T_c among the samples is primarily due to cation nonstoichiometry and not due to differing hole concentrations. Annealing conditions for obtaining optimal (OP), and typical underdoped (UD) and overdoped (OD) samples are listed in Table 1. The results for Bi2201 are on the as-grown crystals and accordingly may not exactly reflect $T_{c,\text{max}}$. However, by carrying out a series of annealing studies, we have confirmed that the systematic change of T_c among our samples is not due to different hole concentrations, but due to the different Ln ions.

Superconducting transition temperatures were determined by AC susceptibility measurements using a Quantum Design Physical Properties Measurement System (PPMS). The transition temperatures reported here correspond to the onset of a diamagnetic signal. We note that the different definition of T_c (such as the intercept between the superconducting transition slope and the $\chi = 0$ axis) does not affect our conclusions due to the sharp superconducting transition (less than 2K for most samples), as shown below. Although it is hard to determine the exact superconducting fraction due to the demagnetization factor of the plate-shaped crystals, the magnitude of the superconducting signal suggests the

TABLE I: Sample preparation conditions and crystal compositions derived from the ICP analysis for Bi2212 single crystals. The ICP analysis on the third sample in the Table was done on cleaved, single-phase samples from an ingot containing a small amount of SrCuO₂ secondary phase.

nominal composition	ICP results	Bi:Sr ratio	growth atmosphere	annealing condition		
				UD	OP	OD
Bi _{2.2} Sr _{1.8} CaCu ₂ O _{8+δ}	Bi _{2.19} Sr _{1.86} Ca _{1.07} Cu ₂ O _{8+δ}	1.178	1atm	700°C	750°C	400°C
			O ₂	air	O ₂	O ₂
Bi _{2.04} Sr _{1.96} CaCu ₂ O _{8+δ}	Bi _{2.06} Sr _{1.93} Ca _{0.96} Cu ₂ O _{8+δ}	1.069	3atm	650°C	500°C	as-grown
			O ₂	Ar	Ar	
Bi _{2.00} Sr _{2.00} CaCu ₂ O _{8+δ}	Bi _{2.06} Sr _{2.04} Ca _{0.87} Cu ₂ O _{8+δ}	1.008	1atm	650°C	500°C	650°C
			O ₂ :Ar=7:93	Ar	Ar	O ₂
Bi _{2.00} Sr _{2.00} Ca _{0.92} Y _{0.08} Cu ₂ O _{8+δ}	Bi _{2.02} Sr _{2.01} Ca _{0.85} Y _{0.08} Cu ₂ O _{8+δ}	1.004	1atm	650°C	400°C	500°C
			O ₂ :Ar=20:80	Ar	Ar	O ₂

bulk superconductivity of the grown samples. No appreciable differences were observed between different samples from the same growth, or between different crystals prepared under identical conditions, an indication of the macroscopic homogeneity of the crystals and the reproducibility of our sample growth process.

III. EXPERIMENTAL RESULTS

A. Results for Bi2201

We have grown a series of Ln³⁺ substituted Bi₂Sr_{1.6}Ln_{0.4}CuO_{6+δ} single crystals with Ln = La, Pr, Nd, Sm, Eu, Gd, Bi. The ionic radius of Ln³⁺ ions, R_{Ln} , decreases monotonically with increasing atomic number, 1.14 Å (La³⁺), 1.06 Å (Pr³⁺), 1.04 Å (Nd³⁺), 1.00 Å (Sm³⁺), 0.98 Å (Eu³⁺), 0.97 Å (Gd³⁺), and 0.96 Å (Bi³⁺)¹¹. Accordingly, by introducing different Ln ions, we can systematically change the ionic radius mismatch between Sr²⁺ (1.12 Å) and Ln³⁺. We use this mismatch, defined as $\Delta R \equiv |R_{Sr} - R_{Ln}|$, to quantify the magnitude of the local lattice distortion around Ln³⁺ ions.

In Fig. 1(a), we show magnetic susceptibility data for a series of Ln³⁺ substituted samples grown under the same conditions. The T_c of the La-doped sample was 33 K with a transition width of less than 1 K, a reasonable result for an as-grown crystal with this composition¹⁰. As shown in Fig. 1(b), T_c decreases monotonically with increasing ΔR , yielding 29 K (Pr³⁺), 27.5 K (Nd³⁺), 23 K (Sm³⁺), 18 K (Eu³⁺), and 12 K (Gd³⁺), respectively. There is no trace of superconductivity down to 1.8 K for the Bi-substituted sample. This is reasonable, since the ionic radius of Bi³⁺ is the smallest of the Ln ions, and the shape of the Bi³⁺ ion tends to be asymmetric due to the presence of a (6s)² lone pair⁸, which might cause additional local lattice distortions. These observations demonstrate the strong sensitivity of T_c to Sr site substitution in Bi2201.

Although one can minimize the magnitude of the local lattice distortion through the choice of the La³⁺ ion,

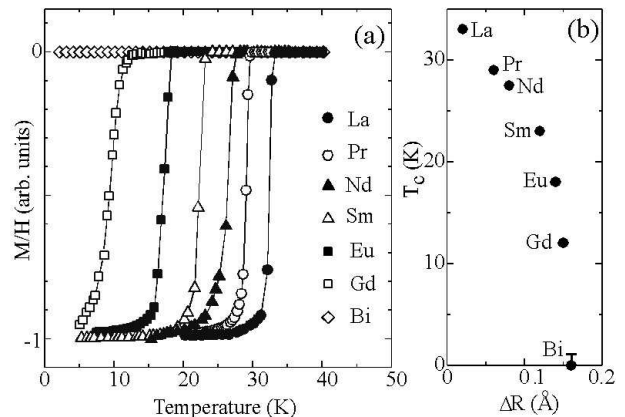


FIG. 1: (a) Bi₂Sr_{1.6}Ln_{0.4}CuO_{6+δ} susceptibility curves, normalized to -1 at the lowest temperature. (b) T_c values as a function of ΔR .

which has a radius similar to that of Sr²⁺, there remains another type of chemical disorder, that is, the random Coulomb potential caused by heterovalent ion substitution. For LSCO, ⁶³Cu NQR spin-lattice relaxation rates experiments have revealed signatures for an electronic inhomogeneity and the results have been discussed in connection with the random distribution of Sr²⁺ ions¹². Considering that both LSCO and Bi2201 contain A-site chemical disorder, it seems likely that the disorder would affect the electronic properties of Bi2201 to a degree comparable to that observed in LSCO, and much more strongly than for the structurally similar material Tl₂Ba₂CuO_{6+δ} (Tl2201) which is believed to be essentially free of A-site disorder. We will discuss this issue in more detail below.

B. Results for Bi2212

Since cation substitution at the Sr site has such a dramatic effect on T_c in Bi2201, in particular for Ln=Bi, one might expect to find similar results for Bi2212. To verify this, we have grown single crystals

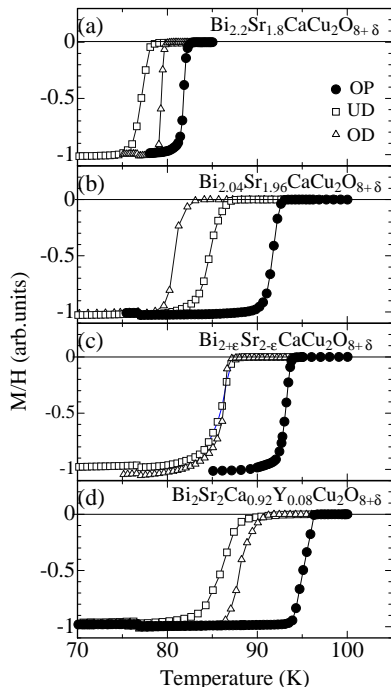


FIG. 2: $\text{Bi}_{2+x}\text{Sr}_{2-x}\text{Ca}_{1-y}\text{Y}_y\text{Cu}_2\text{O}_{8+\delta}$ susceptibility curves, normalized to -1 at the lowest temperature. Data for optimally-doped (OP), underdoped (UD), and overdoped (OD) samples are indicated for each cation composition by closed circles, open squares, and open triangles, respectively.

of $\text{Bi}_{2+x}\text{Sr}_{2-x}\text{CaCu}_2\text{O}_{8+\delta}$. By adopting the methods described in Sec. II, we have managed to grow single crystals over the range $0.0 < x \leq 0.2$. In Figs. 2(a)-(c), we present magnetic susceptibility data for three different crystals with compositions $x = 0.2$, 0.04 , and $\simeq 0$, respectively (ϵ in the chemical formula for the nominal $x = 0$ sample (Fig. 2 (c)) implies the presence of residual nonstoichiometry in our sample, as discussed in the previous section). In the figures, OP indicates optimally-doped samples, which possess $T_{c,\text{max}}$ for a given cation composition. Representative data for underdoped (UD) and overdoped (OD) samples, which were obtained by reducing and oxidizing OP samples, are also plotted to demonstrate successful control of the hole concentration over a wide range.

As the Bi:Sr ratio approaches 1:1, $T_{c,\text{max}}$ increases from 82.4 K for $x = 0.2$, to 91.4 K for $x = 0.07$ (not shown), 92.6 K for $x = 0.04$, and eventually to 94.0 K for the sample closest to the stoichiometric composition that we could grow. We note that most of the samples studied in the literature contain a nonstoichiometry of $x \sim 0.1$ with $T_c = 89 - 91$ K⁹, consistent with the present results.

Although T_c of Bi2212 can be raised by trying to enforce Bi:Sr stoichiometry, the preparation of nearly stoichiometric samples becomes much more difficult than when nonstoichiometry is allowed. This could be due to a

greater stability of the crystal structure when it contains additional positive charges, which are usually introduced by allowing the $\text{Bi}^{3+}:\text{Sr}^{2+}$ ratio to be larger than one, as discussed in Ref. 8. If this is indeed the case, one might expect to be able to synthesize higher- $T_{c,\text{max}}$ samples more easily by introducing extra positive charges via cation substitution that causes disorder less severe than substitution of Bi^{3+} ions at the Sr site.

In the case of Bi2201 we observed that the substitution of additional Ln atoms can eliminate excess Bi atoms from the unfavorable Sr site position, effectively lowering the magnitude of disorder and raising T_c . In the double-layer material Bi2212, there is an additional crystallographic site, the Ca site located between the CuO_2 planes, which can also accept trivalent dopant ions. One might expect Ln^{3+} ions at the Ca site to be a weaker type of disorder than Bi^{3+} ions at the Sr site, since there are no apical oxygens in the Ca planes that could couple to Cu atoms in the CuO_2 planes.

To test this idea we have also grown Y-substituted $\text{Bi}_2\text{Sr}_2\text{Ca}_{1-y}\text{Y}_y\text{Cu}_2\text{O}_{8+\delta}$ crystals. We find that this compound is as easy to prepare as ordinary (nonstoichiometric) Bi2212, and that for Y-Bi2212 the Bi:Sr ratio indeed tends to be stoichiometric. Furthermore, as shown in Fig. 2(d), $T_{c,\text{max}}$ for the $y = 0.08$ sample was increased to 96.0 K, a value higher than for any other Bi2212 sample reported in the literature.⁹ We also grew $y = 0.10$ and $y = 0.12$ samples and confirmed that $T_{c,\text{max}} > 95$ K in both cases.

IV. DISCUSSION

The effect on T_c of structural distortions associated with cation substitution has been extensively studied in LSCO-based materials¹³, and it is established that T_c strongly depends on the A-site (La site) ionic radius mismatch. For instance, Attfield *et al.* used simultaneous co-substitution of several alkaline earth and Ln ions to hold the average A-site ionic radius constant while systematically controlling the variance of the A-site ionic radius, and found that T_c is affected not just by the average radius, but also by the degree of disorder (the variance) at that crystallographic site. Our study of single-layer Bi2201 continues this line of inquiry to a different superconducting material and demonstrates a similar sensitivity of T_c to A-site disorder. We note that our results qualitatively agree with those of a previous study on polycrystalline Bi2201 samples¹⁴.

One can see the same trend in Bi2212 crystals with varying degrees of chemical inhomogeneity. As expected, we find that T_c is strongly dependent on the A-site disorder introduced by the Bi:Sr nonstoichiometry. Furthermore, we also demonstrate that by the seemingly counter-intuitive method of introducing additional Y^{3+} ions, and hence a new type of disorder, we can raise $T_{c,\text{max}}$ to 96 K while minimizing A-site disorder. This suggests that, although the minimization of chemical dis-

order is important for raising T_c , different types of disorder are not equally harmful. This is consistent with the observation¹⁵ that by carefully controlling disorder in the triple-layer material $\text{TlBa}_2\text{Ca}_2\text{Cu}_3\text{O}_{9+\delta}$ (Tl1223) T_c can be raised from ~ 120 K to 133.5 K, a new record for that system, and that Ba site (the A-site in this system) cation disorder (deficiency) has the strongest effect on T_c .

Numerous experiments on Bi2212 have suggested non-uniformity in its electronic properties. These include broad linewidths seen in inelastic neutron scattering experiments¹⁶, residual low-energy excitations in the superconducting state observed in penetration depth measurements¹⁷, finite spin susceptibility at low temperatures observed in NMR studies¹⁸, and short quasiparticle lifetimes detected by complex conductivity experiments¹⁹. The most recent of these are STM/STS measurements² that purport to directly image patch-shaped, electronically inhomogeneous regions. The Bi:Sr nonstoichiometry which inherently exists in most samples may be partially responsible for these experimental observations.

Although the present results do not directly prove the presence of nanoscale electronic inhomogeneity, they can be taken as a circumstantial supporting evidence, since they successfully prove the existence of nanoscale chemical inhomogeneity which potentially pins down electronic inhomogeneity. To explain their STM/STS results, Pan *et al.*² attribute the source of pinning centers to excess oxygen in the BiO planes. Although the overall framework addressed by Pan *et al.* should still hold, we consider that the Bi ions on the Sr site are more effective as pinning centers since they are closer to the CuO_2 planes and affect T_c more directly. Indeed, assuming a random distribution of Bi ions on the Sr site and a nonstoichiometry of $x = 0.10$, the average separation between Bi ions is $\sim 1 - 2$ nm, comparable with the length scale observed in the STM/STS studies.

Recent ^{89}Y NMR experiments on YBCO indicate that the spatial inhomogeneity in this system is much less severe than in LSCO or Bi2212⁵. This is reasonable since the latter two systems exhibit a much higher degree of disorder located at the A-site (La site (LSCO) and Sr site (Bi2212)), whereas YBCO (Ba site) is thought to be free from such cation disorder. Indeed, recent penetration depth measurements on the YBCO variant $\text{Nd}_{1+x}\text{Ba}_{2-x}\text{Cu}_3\text{O}_{7-\delta}$, with cationic disorder at the Ba site, demonstrate that the superconducting properties of this system change quite sensitively with the degree of Nd/Ba nonstoichiometry²⁰.

V. DISORDER EFFECTS IN THE CUPRATES

The two main lessons to be learned from our Bi2201 and Bi2212 case studies are that (1) chemical inhomogeneity affects $T_{c,\text{max}}$ and that (2) the effect of disorder differs depending on its location. In the following, we attempt to classify the various sites at which chemical

disorder is possible and categorize other superconducting families on the basis of which kind of disorder is prevalent in each system.

In Fig. 3, we classify 25 cuprate superconductors based on the pattern of the chemical disorder and the number of CuO_2 planes in the unit cell.²¹ In the first row, we illustrate three possible locations of chemical disorder relative to the CuO_5 pyramids in multilayer materials, or to the CuO_6 octahedra in single-layer materials. Pattern (a) corresponds to the Bi:Sr nonstoichiometry in Bi2201 and Bi2212, or Sr^{2+} ions doped into the La site in LSCO, referred to as A-site disorder so far. The disorder is located next to the apical oxygen. Pattern (b) corresponds to Y^{3+} substitution for Ca^{2+} in Bi2212 and represents disorder located next to the CuO_2 plane, but at a position where there are no apical oxygen atoms with which to bond. There is no corresponding (b) site in single-layer materials. Pattern (c) disorder is further away from the CuO_2 plane. We include excess oxygen δ in Bi- and Tl-based cuprates, oxygen defects in CuO chains in $\text{YBa}_2\text{Cu}_3\text{O}_{7-\delta}$, and Hg deficiency y as well as excess oxygen δ in $\text{Hg}_{1-y}\text{Ba}_2\text{Ca}_{n-1}\text{Cu}_n\text{O}_{2n+2+\delta}$ in this category. We note that the materials are catalogued based on the *primary* form of disorder that they are believed to exhibit.

As demonstrated in the present case study, the effect of the chemical disorder is expected to be stronger for pattern (a) than for pattern (b), which is reasonable considering the role of the apical oxygen atom in passing on the effect of disorder to nearby Cu atoms. First, the random Coulomb potential caused by type (a) disorder changes the energy levels of the apical oxygen orbitals, which can be transmitted to CuO_2 planes through the hybridization between the apical $\text{O}(2p_z)$ orbital and the $\text{Cu}(3d_{7-2-3z^2})$ orbital. Second, the displacement of the apical oxygen caused by type (a) disorder brings about a local lattice distortion to the CuO_2 planes. The effect of pattern (c) disorder is expected to be weakest since the disorder is located relatively far away from the CuO_2 plane.

The number of CuO_2 planes per unit cell may be regarded as another parameter that, in effect, determines the magnitude of the chemical disorder. As demonstrated in Bi2212, multilayer materials can accommodate heterovalent ions by making use of type (b) substitution whose effect on T_c was seen to be weaker than type (a) substitution. Furthermore, the space between the CuO_2 planes forming a multilayer may buffer the impact of the disorder. For instance, in single-layer materials, any displacement of the “upper” apical oxygen in a CuO_6 octahedron creates stress in the CuO_2 plane because the motion of the octahedron is constrained by the “lower” apical oxygen. Double-layer materials contain CuO_5 pyramids rather than CuO_6 octahedra, and the separation between CuO_2 planes relieves this stress, reducing the effects of type (a) disorder. This buffer zone between the outer CuO_2 planes is further increased in triple-layer materials, with the additional benefit that the middle layer is somewhat “protected” from the direct effects of pat-

tern (a) (and (c)) disorder.

Cursory examination of Fig. 3 reveals that $T_{c,max}$ generally increases both across the rows and down the columns of the chart. Indeed, there is no material in (a-1) which possesses a $T_{c,max}$ higher than 50 K. Furthermore, Bi2201 in column (a) has a lower $T_{c,max}$ than Tl2201 in column (c), despite their similar crystal structures. Similarly, $T_{c,max}$ of $TlBa_{1+x}La_{1-x}CuO_5$ (Tl1201) is lower than that of $HgBa_2CuO_{4+\delta}$ (Hg1201).

This trend is closely obeyed when one concentrates on the variation within a single family of materials, each denoted by a different color in the chart. For example, across the first row, oxygen-intercalated $La_2CuO_{4+\delta}$ located in (c-1) has higher $T_{c,max}$ than Sr-substituted La_2CuO_4 (a-1). Down the column, $T_{c,max}$ of the bilayer La-based system $La_{2-x}Sr_xCaCu_2O_6$ (a-2) is higher than that of its single-layer cousin. The classification suggests a negative correlation between the effective magnitude of chemical disorder and $T_{c,max}$. Additional remarks are made in Ref.s 22,23,24.

We note that one may also have to consider other factors which characterize the *global* materials properties and are likely to play a significant role as well in determining $T_{c,max}$, such as Madelung potential²⁶, bond valence sum²⁵, band structure²⁷, block layer²⁸, multi layer²⁹ etc. Although the present scheme is somewhat oversimplified and does not take account of these parameters, we believe it serves as a useful framework within which to consider the chemical disorder effects prevalent in these materials, at least some of which, if ignored, have the potential to lead to the misinterpretation of experimental data. Finally, similar to previous work on Tl1223¹⁵ and to the present work on Bi2212, it might be possible to raise $T_{c,max}$ of certain other cuprates by minimizing the effects of chemical disorder.

VI. SUMMARY

In summary, we present case studies of the effects of chemical disorder on the superconducting transition temperature of the single-layer and double-layer Bi-based cuprate superconductors. We find that the superconducting transition temperature of Bi2212 can be increased up to 96 K by lowering the impact of Sr site disorder, the primary type of disorder inherent to the bismuth family of materials, at the expense of Ca site disorder. Based on these experimental results, we present a qualitative hierarchy of possible disorder sites, and then proceed to categorize the hole-doped high-temperature superconductors on that basis.

Acknowledgments

We thank G. Blumberg, J. Burgy, E. Dagotto, J. C. Davis, D. S. Dessau, T. H. Geballe, E. W. Hudson, A. Iyo, A. Kapitulnik, G. Kinoda, S. A. Kivelson, R. B. Laughlin, B. Y. Mozyzhes, D. J. Scalapino, T. Timusk, and J. M. Tranquada for helpful discussions. This work was supported by the NEDO grant “Nanoscale phenomena of self-organized electrons in complex oxides-new frontiers in physics and devices”, by the U.S. DOE under contract nos. DE-FG03-99ER45773 and DE-AC-03-76SF00515, by NSF DMR9985067, DMR0071897, ONR N00014-98-0195 and by the DOE’s Office of Basic Energy Science, Division of Material Science, Division of Chemical Science, through the Stanford Synchrotron Radiation Laboratory (SSRL). H. Eisaki was supported by the Marvin Chodorow Fellowship in the Department of Applied Physics, Stanford University.

* Present address: Nanoelectronic Research Institute, AIST, Tsukuba 305-8568, Japan

† Present address: National Metrology Institute of Japan, AIST, Tsukuba 305-8568, Japan

‡ Present address: Department of Physics & Astronomy, The University of British Columbia, 334-6224 Agricultural Rd. Vancouver, B.C. V6T 1Z1, Canada and Department of Physics, Fudan University, Shanghai, China

§ Present address: Department of Physics & Astronomy, The University of British Columbia, 334-6224 Agricultural Rd. Vancouver, B.C. V6T 1Z1, Canada

¹ J. M. Tranquada, B. J. Sternlieb, J. D. Axe, Y. Nakamura, and S. Uchida, *Nature* **375**, 561 (1995); J. M. Tranquada, J. D. Axe, N. Ichikawa, A. R. Moodenbaugh, Y. Nakamura, and S. Uchida, *Phys. Rev. Lett.* **78**, 338 (1997).

² S. H. Pan, J. P. O’Neal, R. L. Badzey, C. Chamon, H. Ding, J. R. Engelbrecht, Z. Wang, H. Eisaki, S. Uchida, A. K. Gupta, K. W. Ng, E. W. Hudson, K. M. Lang, and J. C. Davis, *Nature* **413**, 282 (2001); C. Howald, P. Fournier, and A. Kapitulnik, *Phys. Rev. B* **64**, 100504 (2001); K.

M. Lang, V. Madhavan, J. E. Hoffman, E. W. Hudson, H. Eisaki, S. Uchida, and J. C. Davis, *Nature* **415**, 412 (2002); G. Kinoda, T. Hasegawa, S. Nakao, T. Hanaguri, K. Kitazawa, K. Shimizu, J. Shimoyama, and K. Kishio, *Phys. Rev. B* **67**, 224509 (2003); A. Matsuda, T. Fujii, and T. Watababe, *Physica C* **388-389**, 207 (2003); K. Matsuba, H. Sakata, T. Mochiku, K. Hirata, and N. Nishida, *Physica C* **388-389**, 281 (2003).

³ J. Zaanen and O. Gunnarsson, *Phys. Rev. B* **40**, 7391 (1989); S. A. Kivelson, E. Fradkin, and V. J. Emery, *Nature* **393**, 550 (1998); S. R. White and D. J. Scalapino, *Phys. Rev. B* **60**, R753 (1999); J. Burgy, M. Mayr, V. Martin-Mayor, A. Moreo, and E. Dagotto, *Phys. Rev. Lett.* **87**, 277202 (2001); I. Martin and V. Balatsky, *Physica C* **357-360**, 46 (2001).

⁴ B. G. Levi, *Physics Today*, **51**, No. 6, 19 (1998); J. Orenstein and A. J. Millis, *Science* **288**, 468 (2000); J. W. Loram, J. L. Tallon, and W. Y. Liang, *cond-mat/0212461*.

⁵ J. Bobroff, H. Alloul, S. Ouazi, P. Mendels, A. Mahajan, N. Blanchard, G. Collin, V. Guillen, and J.-F. Marucco,

- Phys. Rev. Lett. **89**, 157002 (2002).
- 6 A. Damascelli, Z.-X. Shen, and Z. Hussain, Rev. Mod. Phys. **75**, 473 (2003).
 - 7 Y. Ikeda, H. Ito, S. Shimomura, Y. Oue, K. Inaba, Z. Hiroi, and M. Takano, Physica C **159**, 93 (1989); A. Maeda, M. Hase, I. Tsukada, K. Noda, S. Takebayashi, and K. Uchinokura, Phys. Rev. B **41**, 6418 (1990).
 - 8 H. E. Zandbergen, W. A. Groen, A. Smit, and G. Vantendelo, Physica C **168**, 426 (1990).
 - 9 (a). Bi_{2.10}Sr_{1.94}Ca_{0.88}Cu_{2.07}O_y, T_c=90K; D. B. Mitzi, L. W. Lombardo, A. Kapitulnik, S. S. Laderman, and R. D. Jacowitz, Phys. Rev. B **41**, 6564 (1990).
 (b). Bi_{2.04}Sr_{1.93}Ca_{0.92}Cu_{2.02}O_y, T_c=88K, C. Kendziora, M. C. Martin, J. Hartge, L. Mihaly, and L. Forro, Phys. Rev. B **48**, 3531 (1993).
 (c). Bi_{2.03}Sr_{1.74}Ca_{1.08}Cu_{2.05}O_y, T_c=92K; T. Mochiku and K. Kadowaki, Physica C **235-240**, 523 (1994).
 (d). Bi_{2.14}Sr_{1.77}Ca_{0.92}Cu_{2.00}O_y, T_c=93K, Y. Kotaka, T. Kimura, H. Ikuta, J. Shimoyama, K. Kitazawa, K. Yamafuji, K. Kishio, and D. Pooke, Physica C **235-240**, 1529 (1994).
 (e). Bi_{2.05}Sr_{1.79}Ca_{0.93}Cu_{2.00}O_x, T_c=92K; G. D. Gu, T. Egi, N. Koshizuka, P. A. Miles, G. J. Russell, and S. J. Kennedy, Physica C **263**, 180 (1996).
 (f). Bi_{2.1}Sr_{1.9}CaCu₂O_y, T_c=89-90K; T. Watanabe, T. Fujii, and A. Matsuda, Phys. Rev. Lett. **79**, 2113 (1997).
 (g). "nearly perfect stoichiometric", T_c=95K, M. Rübhausen, P. Guptasarma, D. G. Hinks, and M. V. Klein, Phys. Rev. B **58**, 3462 (1998).
 (h). Bi_{2.15}Sr_{1.85}CaCu₂O_y, T_c=90K, J. W. Loram, J. L. Luo, J. R. Cooper, W. Y. Liang, and J. L. Tallon, Physica C **341-348**, 831 (2000).
 (i). Bi_{2.10}Sr_{1.90}Ca_{1.0}Cu_{2.0}O_y, T_c=95K, A. Maljuk, B. Liang, C. T. Lin, and G. A. Emelchenko, Physica C **355**, 140 (2001).
 - 10 Y. Ando and T. Murayama, Phys. Rev. B **60**, R6991 (1999); S. Ono, Y. Ando, T. Murayama, F. F. Balakirev, J. B. Betts, and G. S. Boebinger, Phys. Rev. Lett. **85**, 638 (2000); Y. Wang and N. P. Ong, Proc. Nat. Acad. Sci. USA, **98**, 11091 (2001).
 - 11 In this paper we use the ionic radii shown in L. H. Ahrens, Geochim Cosmochim Acta **2**, 155 (1952).
 - 12 S. Fujiyama, Y. Ito, H. Yasuoka, and Y. Ueda, J. Phys. Soc. Jpn, **66**, 2864 (1997) ; P. M. Singer, A. W. Hunt, and T. Imai, Phys. Rev. Lett. **88**, 047602 (2002); P. M. Singer, A. W. Hunt, and T. Imai, cond-mat/0302077.
 - 13 J. D. Axe, A. H. Moudden, D. Hohlwein, D. E. Cox, K. M. Mohanty, A. R. Moodenbaugh, and Y. Xu, Phys. Rev. Lett. **62**, 2751 (1989); M. K. Crawford, R. L. Harlow, E. M. McCarron, W. E. Farneth, J. D. Axe, H. Chou, and Q. Huang, Phys. Rev. B **44**, 7749 (1991); K. Yoshida, F. Nakamura, Y. Tanaka, Y. Maeno, and T. Fujita, Physica C **230**, 371 (1994); B. Büchner, M. Breuer, A. Freimuth, and A. P. Kampf, Phys. Rev. Lett. **73**, 1841 (1994); B. Dabrowski, Z. Wang, K. Rogacki, J. D. Jorgensen, R. L. Hitterman, J. L. Wagner, B. A. Hunter, P. G. Radaelli, and D. G. Hinks, Phys. Rev. Lett. **76**, 1348 (1996); J.P. Attfield, A.L. Kharlanov, and J.A. McAllister, Nature **394**, 157 (1998).
 - 14 H. Nameki, M. Kikuchi, and Y. Syono, Physica C **234** 255 (1994).
 - 15 A. Iyo, Y. Tanaka, Y. Ishiura, M. Tokumoto, K. Tokiwa, T. Watanabe, and H. Ihara, Supercond. Sci. Technol. **14**, 504 (2001); H. Kotegawa, Y. Tokunaga, K. Ishida, G.-q. Zheng, Y. Kitaoka, A. Iyo, Y. Tanaka, and H. Ihara, Phys. Rev. B **65**, 184504 (2002).
 - 16 H. F. Fong, P. Bourges, Y. Sidis, L. P. Regnault, A. Ivanov, G. D. Gu, N. Koshizuka, and B. Keimer, Nature **398**, 588 (1999).
 - 17 A. Maeda, T. Shibauchi, N. Kondo, K. Uchinokura, and M. Kobayashi, Phys. Rev. B **46**, 14234 (1992).
 - 18 M. Takigawa and D. B. Mitzi, Phys. Rev. Lett. **73**, 1287 (1994).
 - 19 J. Corson, J. Orenstein, S. Oh, J. O'Donnell, and J. N. Eckstein, Phys. Rev. Lett. **85**, 2569 (2000).
 - 20 M. Salluzzo, F. Palomba, G. Pica, A. Andreone, I. Maggio-Aprile, O. Fischer, C. Cantoni, and D. P. Norton, Phys. Rev. Lett. **85**, 1116 (2000).
 - 21 (a-1) Ca_{2-x}Na_xCuO₂Cl₂, Z. Hiroi, N. Kobayashi, and M. Takano, Nature **371**, 139 (1994).
 (a-1) Pb₂Sr_{2-x}La_xCu₂O_z, H. Sasakura, K. Nakahigashi, S. Minamigawa, S. Nakanishi, M. Kogachi, N. Fukuoka, M. Yoshikawa, S. Noguchi, K. Okuda, and A. Yanase, Jpn. J. Appl. Phys. **29**, L583 (1990).
 (a-1) La_{2-x}Sr_xCuO₄, H. Takagi, R. J. Cava, M. Marezio, B. Batlogg, J. J. Krajewski, W. F. Peck, Jr., P. Bordet, and D. E. Cox, Phys. Rev. Lett. **68**, 3777 (1992).
 (a-1) Bi₂Sr_{1-x}Ln_xCuO_{6+δ}, S. Ono, Y. Ando, T. Murayama, F. F. Balakirev, J. B. Betts, and G. S. Boebinger, Phys. Rev. Lett. **85**, 638 (2000).
 (a-1) TlBa_{1+x}La_{1-x}CuO₅, T. Manako and Y. Kubo, Phys. Rev. B **50**, 6402 (1994).
 (c-1) Sr₂CuO₂F_{2+x}, M. Al-Mamouri, P. P. Edwards, C. Greaves, and M. Slaski, Nature **369**, 382 (1994).
 (c-1) La₂CuO_{4+δ}, F.C. Chou, J. H. Cho and D.C. Johnston, Physica C **197**, 303 (1992).
 (c-1) Tl₂Ba₂CuO_{6+δ}, J. L. Wagner, O. Chmaissem, J. D. Jorgensen, D. G. Hinks, P. G. Radaelli, B. A. Hunter, and W. R. Jensen, Physica C **277**, 170 (1997).
 (c-1) HgBa₂CuO_{4+δ}, A. Yamamoto, K. Minami, W.-Z. Hu, A. Miyakita, M. Izumi, and S. Tajima, Phys. Rev. B **65**, 104505 (2002).
 (a-2) La_{2-x}Sr_xCaCu₂O₆, R. J. Cava, B. Batlogg, R. B. van Dover, J. J. Krajewski, J. V. Waszczak, R. M. Fleming, W. F. Peck, L. W. Rupp, P. Marsh, A. C. W. P. James, and L. F. Schneemeyer, Nature **345**, 602 (1990).
 (a-2) (La_{1-x}Ca_x)(Ba_{1.75-x}La_{0.25+x})Cu₃O_y, O. Chmaissem, J. D. Jorgensen, S. Short, A. Knizhnik, Y. Eckstein, and H. Shaked, Nature **397**, 45 (1999).
 (a-2) Bi_{2+x}Sr_{2-x}CaCu₂O_{8+δ}, Ref. 9
 (b-2) Pb₂Sr₂Y_{1-x}Ca_xCu₃O_{8+δ}, Y. Koike, M. Masuzawa, T. Noji, H. Sunagawa, H. Kawabe, N. Kobayashi, and Y. Saito, Physica C **170**, 130 (1990).
 (b-2) Y_{1-x}Ca_xBa₂Cu₃O_{7-δ}, J. L. Tallon, C. Bernhard, H. Shaked, R. L. Hitterman, and J. D. Jorgensen, Phys. Rev. B **51**, 12911 (1995).
 (b-2) Bi₂Sr₂Ca_{1-x}Y_xCu₂O_{8+δ}, this work.
 (c-2) YBa₂Cu₃O_{7-δ}, R. Liang, D. A. Bonn, and W. N. Hardy, Physica C **304**, 105 (1998).
 (c-2) TlBa₂CaCu₂O_{7+δ}, S. Nakajima, M. Kikuchi, Y. Syono, K. Nagase, T. Oku, N. Kobayashi, D. Shindo, and K. Hiraga, Physica C **170**, 443 (1990).
 (c-2) Tl₂Ba₂CaCu₂O_{8+δ}, Y. Shimakawa, Y. Kubo, T. Manako, and H. Igarashi, Phys. Rev. B **40**, 11400 (1989).
 (c-2) HgBa₂CaCu₂O_{6+δ}, R. L. Meng, L. Beauvais, X. N. Zhang, Z. J. Huang, Y. Y. Sun, Y. Y. Xue, and C. W. Chu, Physica C **216**, 21 (1993).
 (a-3) Bi_{2+x}Sr_{2-x}Ca₂Cu₃O_{10+δ}, J. M. Tarascon, W. R.

McKinnon, P. Barbour, D. M. Hwang, B. G. Bagley, L. H. Greene, G. W. Hull, Y. LePage, N. Stoffel, and M. Giroud, *Phys. Rev. B* **38**, 8885 (1988).

(a-3) $\text{TlBa}_{2-\epsilon}\text{Ca}_2\text{Cu}_3\text{O}_{9+\delta}$, A. Iyo, Y. Tanaka, Y. Ishiura, M. Tokumoto, K. Tokiwa, T. Watanabe, and H. Ihara, *Supercond. Sci. Technol.* **14**, 504 (2001).

(b-3) $\text{TlBa}_2\text{Ca}_{2-\epsilon}\text{Cu}_3\text{O}_{9+\delta}$, same as above.

(c-3) $\text{TlBa}_2\text{Ca}_2\text{Cu}_3\text{O}_{9+\delta}$, same as above.

(c-3) $\text{Tl}_2\text{Ba}_2\text{Ca}_2\text{Cu}_3\text{O}_{10+\delta}$, Y. Shimakawa, Y. Kubo, T. Manako, and H. Igarashi, *Phys. Rev. B* **40**, 11400 (1989).

(c-3) $\text{HgBa}_2\text{Ca}_2\text{Cu}_3\text{O}_{8+\delta}$, R. L. Meng, L. Beauvais, X. N. Zhang, Z. J. Huang, Y. Y. Sun, Y. Y. Xue and C. W. Chu, *Physica C* **216**, 21 (1993).

Besides those listed in Fig. 3, many materials may be classified within the present framework. Examples are;

(I) Infinite layered material $(\text{Sr}_{1-x}\text{Ca}_x)_{1-y}\text{CuO}_2$ with $T_{c,\text{max}}=110$ K (M. Azuma, Z. Hiroi, M. Takano, Y. Bando, and Y. Takeda, *Nature* **356**, 775 (1992)), which can be described as (b- ∞).

(II) Electron doped superconductor, $\text{Ln}_{2-x}\text{Ce}_x\text{CuO}_{4-\delta}$ (Ln=Pr, Nd, Sm, $T_{c,\text{max}}=24$ K for Nd) (Y. Tokura, H. Takagi, and S. Uchida, *Nature* **337**, 345 (1989)) is similar to (a-1) since the CuO_2 planes are sandwiched by two LnO planes containing Ce^{4+} ions at the Ln^{3+} site.

(III) T^* compounds and its derivatives, $\text{Nd}_{2-x-y}\text{Ce}_y\text{Sr}_x\text{CuO}_4$ ($T_{c,\text{max}}=22\text{K}$) (H. Sawa, S. Suzuki, M. Watanabe, J. Akimitsu, H. Matsubara, H. Watabe, S. Uchida, K. Kokusho, H. Asano, F. Izumi, and E. Takayama-Muromachi, *Nature* **337**, 347 (1989)), $\text{La}_{1-x-z}\text{Ln}_{1-x}\text{Sr}_z\text{CuO}_4$ ($T_{c,\text{max}}=20\text{K}$ for Ln=Sm) (Y. Tokura, H. Takagi, H. Watabe, H. Matsubara, S. Uchida, K. Hiraga, T. Oku, T. Mochiku, and H. Asano, *Phys. Rev. B* **40**, 2568 (1989)), $(\text{Ln}_{1-x}\text{Ce}_x)_2(\text{Ba}_{1-y}\text{Ln}_y)_2\text{Cu}_3\text{O}_{10-\delta}$ ($T_{c,\text{max}}=33\text{K}$ for Ln=Eu) (H. Sawa, K. Obara, J. Akimitsu, Y. Matsui, and S. Horiuchi, *J. Phys. Soc. Jpn.* **58**, 2252 (1989)), $\text{Bi}_2\text{Sr}_2(\text{Ln}_{1-x}\text{Ce}_x)_2\text{Cu}_2\text{O}_{10+y}$ ($T_{c,\text{max}}=30$ K for Ln=Gd) (Y. Tokura, T. Arima, H. Takagi, S. Uchida, T. Ishigaki, H. Asano, R. Beyers, A. I. Nazzal, P. Lacorre, and J. B. Torrance, *Nature* **342**, 890 (1989)). These materials possess CuO_5 units which are sandwiched by planes containing cation disorders (for example, Nd(Ce)O and Sr(Nd)O planes for $\text{Nd}_{2-x-y}\text{Ce}_y\text{Sr}_x\text{CuO}_4$), and can be classified as (a-1) materials.

²² $\text{YBa}_2\text{Cu}_4\text{O}_8$ has a relatively low T_c of 81 K, although this material is essentially free from chemical disorder (J. Karpinski, E. Kaldis, E. Jilek, S. Rusiecki, and B. Bucher, *Nature* **336**, 660 (1988)). It is known that pure $\text{YBa}_2\text{Cu}_4\text{O}_8$ is underdoped and that its T_c increases to 90 K when Ca is substituted on the Y site (T. Miyatake,

S. Gotoh, N. Koshizuka, and S. Tanaka, *Nature* **341**, 41 (1989); T. Machi, I. Tomeno, K. Tai, N. Koshizuka, and H. Yasuoka, *Physica C* **226**, 227 (1994)), which provides additional holes and makes the system optimally doped, but also increases the amount of chemical disorder. Similarly, stoichiometric $\text{YBa}_2\text{Cu}_3\text{O}_{7-\delta}$ ($\delta = 0.01$, $T_c = 88.5$ K) is slightly overdoped, and $T_{c,\text{max}} = 93.7$ K is found for $\delta \approx 0.07$ ²¹.

²³ It is empirically known that materials with longer Cu-apical oxygen bonds tend to have higher values of T_c . Indeed, in Fig. 3, materials possessing type (a) disorder tend to contain Sr^{2+} ions (1.12 Å) or La^{3+} ions (1.14 Å), whereas those with type (c) disorder possess Ba^{2+} ions (1.34 Å) on the A-site. In the present framework, this tendency can be explained as follows. First, long Cu-apical oxygen bond lengths help to isolate CuO_2 planes from the outer layers which may contain disorder. Second, due to the large difference in the ionic radii of Ba^{2+} (1.34 Å) and other constituent cations such as Ln^{3+} , Bi^{3+} , or Tl^{3+} (0.95 Å), their intersubstitution is usually more difficult than the Bi:Sr intersubstitution seen in the Bi-based compounds, thus making Ba-based materials resistant to type (a) disorder. A good example of this concept is $\text{LnBa}_2\text{Cu}_3\text{O}_7$. Due to the large ionic radius mismatch, Ln and Ba ions usually do not mix with each other. However, for Ln=La and Nd, Ln:Ba intersubstitution is allowed since the mismatch is less severe. $T_{c,\text{max}}$ of the nonstoichiometric $\text{Ln}_{1+x}\text{Ba}_{2-x}\text{Cu}_3\text{O}_7$ is lower than for other members of the series (T. Wada, N. Suzuki, A. Maeda, T. Yabe, K. Uchinokura, S. Uchida, and S. Tanaka, *Phys. Rev. B* **39**, 9126 (1989), Ref. 20), although its average Cu-apical oxygen bond length is longer.

²⁴ For multilayer materials, $T_{c,\text{max}}$ typically increases up to $n = 3$ and then decreases for $n > 3$ (S. Adachi et al., in *Structures of High-Temperature Superconductors*, edited by A. V. Narlikar (Nova Science Publishers, New York, 1997), Vol. 23, pp.163-191). This may be because the benefit of the buffering effect due to the existence of multilayer is saturated in $n=3$.

²⁵ M. H. Whangbo and C. C. Torardi, *Science* **249**, 1143 (1990); J. Tallon, *Physica C* **168**, 85 (1990).

²⁶ Y. Ohta, T. Tohyama, and S. Maekawa, *Phys. Rev. B* **43**, 2968 (1991).

²⁷ E. Pavarini, I. Dasgupta, T. Saha-Dasgupta, O. Jepsen, and O. K. Andersen, *Phys. Rev. Lett.* **87**, 047003 (2001).

²⁸ T. H. Geballe and B. Y. Mozyzhes, *Physica C* **341-348**, 1821 (2000).

²⁹ S. A. Kivelson, *Physica B* **318**, 61 (2002).

Halogen Family	Bi Family	(a)	(b)	(c)																										
Pb Family	1L Tl Family																													
La Family	2L Family	(1) 	(a-1) 	(c-1) 																										
YBCO Family	Hg Family																													
		<table border="1"> <thead> <tr> <th></th> <th>T_c</th> </tr> </thead> <tbody> <tr> <td>$\text{Ca}_{2-x}\text{Na}_x\text{CuO}_2\text{Cl}_2$</td> <td>26</td> </tr> <tr> <td>$\text{Pb}_2\text{Sr}_{2-x}\text{La}_x\text{Cu}_2\text{O}_z$</td> <td>33</td> </tr> <tr> <td>$\text{La}_{2-x}\text{M}_x\text{CuO}_4$</td> <td>39</td> </tr> <tr> <td>$\text{Bi}_2\text{Sr}_{1-x}\text{Ln}_x\text{CuO}_{8+\delta}$</td> <td>38</td> </tr> <tr> <td>$\text{TlBa}_{1+x}\text{La}_{1-x}\text{CuO}_5$</td> <td>45</td> </tr> </tbody> </table>		T_c	$\text{Ca}_{2-x}\text{Na}_x\text{CuO}_2\text{Cl}_2$	26	$\text{Pb}_2\text{Sr}_{2-x}\text{La}_x\text{Cu}_2\text{O}_z$	33	$\text{La}_{2-x}\text{M}_x\text{CuO}_4$	39	$\text{Bi}_2\text{Sr}_{1-x}\text{Ln}_x\text{CuO}_{8+\delta}$	38	$\text{TlBa}_{1+x}\text{La}_{1-x}\text{CuO}_5$	45		<table border="1"> <thead> <tr> <th></th> <th>T_c</th> </tr> </thead> <tbody> <tr> <td>$\text{Sr}_2\text{CuO}_2\text{F}_{2+2x}$</td> <td>46</td> </tr> <tr> <td>$\text{La}_2\text{CuO}_{4+\delta}$</td> <td>45</td> </tr> <tr> <td>$\text{Tl}_2\text{Ba}_2\text{CuO}_{8+\delta}$</td> <td>93</td> </tr> <tr> <td>$\text{HgBa}_2\text{CuO}_{4+\delta}$</td> <td>98</td> </tr> </tbody> </table>		T_c	$\text{Sr}_2\text{CuO}_2\text{F}_{2+2x}$	46	$\text{La}_2\text{CuO}_{4+\delta}$	45	$\text{Tl}_2\text{Ba}_2\text{CuO}_{8+\delta}$	93	$\text{HgBa}_2\text{CuO}_{4+\delta}$	98				
	T_c																													
$\text{Ca}_{2-x}\text{Na}_x\text{CuO}_2\text{Cl}_2$	26																													
$\text{Pb}_2\text{Sr}_{2-x}\text{La}_x\text{Cu}_2\text{O}_z$	33																													
$\text{La}_{2-x}\text{M}_x\text{CuO}_4$	39																													
$\text{Bi}_2\text{Sr}_{1-x}\text{Ln}_x\text{CuO}_{8+\delta}$	38																													
$\text{TlBa}_{1+x}\text{La}_{1-x}\text{CuO}_5$	45																													
	T_c																													
$\text{Sr}_2\text{CuO}_2\text{F}_{2+2x}$	46																													
$\text{La}_2\text{CuO}_{4+\delta}$	45																													
$\text{Tl}_2\text{Ba}_2\text{CuO}_{8+\delta}$	93																													
$\text{HgBa}_2\text{CuO}_{4+\delta}$	98																													
		(2)  	(a-2)  	(b-2)  	(c-2)  																									
		<table border="1"> <thead> <tr> <th></th> <th>T_c</th> </tr> </thead> <tbody> <tr> <td>$\text{La}_{2-x}\text{Sr}_x\text{CaCu}_2\text{O}_6$</td> <td>60</td> </tr> <tr> <td>$(\text{La}_{1-x}\text{Ca}_x)(\text{Ba}_{1.75-x}\text{La}_{0.25+x})\text{Cu}_3\text{O}_y$</td> <td>80</td> </tr> <tr> <td>$\text{Bi}_{2+x}\text{Sr}_{2-x}\text{CaCu}_2\text{O}_{8+\delta}$</td> <td>90</td> </tr> </tbody> </table>		T_c	$\text{La}_{2-x}\text{Sr}_x\text{CaCu}_2\text{O}_6$	60	$(\text{La}_{1-x}\text{Ca}_x)(\text{Ba}_{1.75-x}\text{La}_{0.25+x})\text{Cu}_3\text{O}_y$	80	$\text{Bi}_{2+x}\text{Sr}_{2-x}\text{CaCu}_2\text{O}_{8+\delta}$	90	<table border="1"> <thead> <tr> <th></th> <th>T_c</th> </tr> </thead> <tbody> <tr> <td>$\text{Pb}_2\text{Sr}_2\text{Y}_{1-x}\text{Ca}_x\text{Cu}_3\text{O}_{8+\delta}$</td> <td>80</td> </tr> <tr> <td>$\text{Y}_{1-x}\text{Ca}_x\text{Ba}_2\text{Cu}_3\text{O}_{7-\delta}$</td> <td>90</td> </tr> <tr> <td>$\text{Bi}_2\text{Sr}_2\text{Ca}_{1-x}\text{Y}_x\text{Cu}_3\text{O}_{8+\delta}$</td> <td>96</td> </tr> </tbody> </table>		T_c	$\text{Pb}_2\text{Sr}_2\text{Y}_{1-x}\text{Ca}_x\text{Cu}_3\text{O}_{8+\delta}$	80	$\text{Y}_{1-x}\text{Ca}_x\text{Ba}_2\text{Cu}_3\text{O}_{7-\delta}$	90	$\text{Bi}_2\text{Sr}_2\text{Ca}_{1-x}\text{Y}_x\text{Cu}_3\text{O}_{8+\delta}$	96	<table border="1"> <thead> <tr> <th></th> <th>T_c</th> </tr> </thead> <tbody> <tr> <td>$\text{YBa}_2\text{Cu}_3\text{O}_{7-\delta}$</td> <td>93</td> </tr> <tr> <td>$\text{TlBa}_2\text{CaCu}_2\text{O}_{7+\delta}$</td> <td>110</td> </tr> <tr> <td>$\text{Tl}_2\text{Ba}_2\text{CaCu}_2\text{O}_{8+\delta}$</td> <td>110</td> </tr> <tr> <td>$\text{HgBa}_2\text{CaCu}_2\text{O}_{8+\delta}$</td> <td>120</td> </tr> </tbody> </table>		T_c	$\text{YBa}_2\text{Cu}_3\text{O}_{7-\delta}$	93	$\text{TlBa}_2\text{CaCu}_2\text{O}_{7+\delta}$	110	$\text{Tl}_2\text{Ba}_2\text{CaCu}_2\text{O}_{8+\delta}$	110	$\text{HgBa}_2\text{CaCu}_2\text{O}_{8+\delta}$	120
	T_c																													
$\text{La}_{2-x}\text{Sr}_x\text{CaCu}_2\text{O}_6$	60																													
$(\text{La}_{1-x}\text{Ca}_x)(\text{Ba}_{1.75-x}\text{La}_{0.25+x})\text{Cu}_3\text{O}_y$	80																													
$\text{Bi}_{2+x}\text{Sr}_{2-x}\text{CaCu}_2\text{O}_{8+\delta}$	90																													
	T_c																													
$\text{Pb}_2\text{Sr}_2\text{Y}_{1-x}\text{Ca}_x\text{Cu}_3\text{O}_{8+\delta}$	80																													
$\text{Y}_{1-x}\text{Ca}_x\text{Ba}_2\text{Cu}_3\text{O}_{7-\delta}$	90																													
$\text{Bi}_2\text{Sr}_2\text{Ca}_{1-x}\text{Y}_x\text{Cu}_3\text{O}_{8+\delta}$	96																													
	T_c																													
$\text{YBa}_2\text{Cu}_3\text{O}_{7-\delta}$	93																													
$\text{TlBa}_2\text{CaCu}_2\text{O}_{7+\delta}$	110																													
$\text{Tl}_2\text{Ba}_2\text{CaCu}_2\text{O}_{8+\delta}$	110																													
$\text{HgBa}_2\text{CaCu}_2\text{O}_{8+\delta}$	120																													
		(3)   	(a-3)   	(b-3)   	(c-3)   																									
		<table border="1"> <thead> <tr> <th></th> <th>T_c</th> </tr> </thead> <tbody> <tr> <td>$\text{Bi}_{2+x}\text{Sr}_{2-x}\text{Ca}_2\text{Cu}_3\text{O}_{10+\delta}$</td> <td>110</td> </tr> <tr> <td>$\text{TlBa}_{2-x}\text{Ca}_2\text{Cu}_3\text{O}_{9+\delta}$</td> <td>123</td> </tr> </tbody> </table>		T_c	$\text{Bi}_{2+x}\text{Sr}_{2-x}\text{Ca}_2\text{Cu}_3\text{O}_{10+\delta}$	110	$\text{TlBa}_{2-x}\text{Ca}_2\text{Cu}_3\text{O}_{9+\delta}$	123	<table border="1"> <thead> <tr> <th></th> <th>T_c</th> </tr> </thead> <tbody> <tr> <td>$\text{TlBa}_2\text{Ca}_{2-x}\text{Cu}_3\text{O}_{9+\delta}$</td> <td>131</td> </tr> </tbody> </table>		T_c	$\text{TlBa}_2\text{Ca}_{2-x}\text{Cu}_3\text{O}_{9+\delta}$	131	<table border="1"> <thead> <tr> <th></th> <th>T_c</th> </tr> </thead> <tbody> <tr> <td>$\text{TlBa}_2\text{Ca}_2\text{Cu}_3\text{O}_{9+\delta}$</td> <td>133</td> </tr> <tr> <td>$\text{Tl}_2\text{Ba}_2\text{Ca}_2\text{Cu}_3\text{O}_{10+\delta}$</td> <td>125</td> </tr> <tr> <td>$\text{HgBa}_2\text{Ca}_2\text{Cu}_3\text{O}_{10+\delta}$</td> <td>135</td> </tr> </tbody> </table>		T_c	$\text{TlBa}_2\text{Ca}_2\text{Cu}_3\text{O}_{9+\delta}$	133	$\text{Tl}_2\text{Ba}_2\text{Ca}_2\text{Cu}_3\text{O}_{10+\delta}$	125	$\text{HgBa}_2\text{Ca}_2\text{Cu}_3\text{O}_{10+\delta}$	135								
	T_c																													
$\text{Bi}_{2+x}\text{Sr}_{2-x}\text{Ca}_2\text{Cu}_3\text{O}_{10+\delta}$	110																													
$\text{TlBa}_{2-x}\text{Ca}_2\text{Cu}_3\text{O}_{9+\delta}$	123																													
	T_c																													
$\text{TlBa}_2\text{Ca}_{2-x}\text{Cu}_3\text{O}_{9+\delta}$	131																													
	T_c																													
$\text{TlBa}_2\text{Ca}_2\text{Cu}_3\text{O}_{9+\delta}$	133																													
$\text{Tl}_2\text{Ba}_2\text{Ca}_2\text{Cu}_3\text{O}_{10+\delta}$	125																													
$\text{HgBa}_2\text{Ca}_2\text{Cu}_3\text{O}_{10+\delta}$	135																													

FIG. 3: (Color) Classification of bulk high- T_c cuprates in terms of the disorder site and the number of CuO_2 layers. Materials belonging to the same family are indicated by the same color. Halogen family denotes $(\text{Ca},\text{Sr})_2\text{CuO}_2\text{A}_2$ ($\text{A}=\text{Cl}, \text{F}$) based materials. Bi family denotes $\text{Bi}22(n-1)n$ ($n=1,2,3$). Pb family denotes $\text{Pb}_2\text{Sr}_2\text{Ca}_{n-1}\text{Cu}_{n+1}\text{O}_z$. 1L Tl family denotes one-Tl-layer cuprates, $\text{TlBa}_2\text{Ca}_{n-1}\text{Cu}_n\text{O}_{3+2n+\delta}$. 2L Tl family denotes two-Tl-layer cuprates, $\text{Tl}_2\text{Ba}_2\text{Ca}_{n-1}\text{Cu}_n\text{O}_{4+2n+\delta}$. La family denotes $\text{La}_2\text{Ca}_{n-1}\text{Cu}_n\text{O}_{2+2n}$. YBCO family denotes $\text{LnBa}_2\text{Cu}_3\text{O}_{6+\delta}$. Hg family denotes $\text{HgBa}_2\text{Ca}_{n-1}\text{Cu}_n\text{O}_{2+2n+\delta}$. The transition temperatures are compiled from works listed in Ref. 21